This is a repository copy of *Dye conjugation to linseed oil by highly-effective thiol-ene coupling and subsequent esterification reactions*.

White Rose Research Online URL for this paper:
http://eprints.whiterose.ac.uk/88784/

Version: Accepted Version

Article:

Title: Dye conjugation to linseed oil by highly-effective thiol-ene coupling and subsequent esterification reactions

Authors: Toshiki Hayashi, Algy Kazlauciunas, Paul D. Thornton

Email: paul.d.thornton@leeds.ac.uk
Telephone: +44 (0)113 343 2935
Fax: +44 (0)113 343 6565

ABSTRACT: Linseed oil, a renewable material obtained from the ripened seeds of the flax plant, was conjugated with C. I. Disperse Red 1 to yield a coloured macromolecule in two experimentally-simplistic coupling steps. Firstly, the abundant presence of carbon-carbon double bonds in linseed oil was exploited to introduce carboxylic acid functionality to linseed oil via a thiol-ene reaction between linseed oil and 3-mercaptopropionic acid. C. I. Disperse Red 1 was then grafted to the carboxylic acid units now present via esterification, offering a coloured product in high yields. On average, 39.1% of the carbon-carbon double bonds in each linseed oil molecule were furnished with a C. I. Disperse Red 1 molecule. The remaining carbon-carbon double bonds may therefore be further exploited for chemical crosslinking, ensuring that the product formed is of potential significance as a coloured, bio-based, surface coating product.

1. Introduction

Plant oils are naturally occurring molecules that offer several advantageous features including renewability, biodegradability and cost-effective production. The positive environmental and economic attributes of plant oils have been utilised to synthesise polymers including polyurethanes [1, 2] and polyesters [2, 3]. Additionally, plant oils have been exploited in the creation of numerous products including coatings and inks [4, 5, 6, 7, 8], liquid resin moulds [9, 10], plasticisers [10, 11], hardeners [12, 13], diluents [14], lubricants [15, 16], and emollients [17].

The main component of plant oil is a triglyceride molecule that possesses a structure consisting of three linear fatty acid chains that are conjugated to a glycerine molecule by ester bonds [10]. The fatty acid chains are derived from various fatty acids; plant oils have a distinctive composition depending on the plant from which they are obtained and the growing conditions of the plant [10, 18]. We are particularly interested in utilising linseed oil (**1**) (Fig. 1) for the development coloured, bio-derived coatings. Linseed oil is a drying oil, in which each triglyceride molecule contains 6.6 carbon-carbon double (C=C) bonds on average [10]. This plays a vital role in enabling the oil to dry via auto-oxidation [19, 20]. Linseed oil contains fatty acid chains derived from linolenic acid (18:3, 56.6%), oleic acid (18:1, 19.1%), linoleic acid (18:2, 15.3%), palmitic acid (16:0, 5.5%), and stearic acid (18:0, 3.5%) [10], where the figures in the brackets signify the number of carbon atoms in each fatty acid chain versus the number of C=C bonds, and the content ratio of each fatty acid chain present in linseed oil, respectively. The abundant linolenic acid content of oil promotes its relatively fast drying (or hardening) and suitability to be exploited as a coating product.

The chemical modification of plant oil [10, 21, 22, 23, 24] may be conducted on several sites present within the chemical structure of the oil including C=C bonds, allylic carbons, ester bonds, and the α-carbon of the ester bonds [10]. Although a limited number of plant oils possess additional functionality, for example the alcohol groups that are present in castor oil [25], the introduction of reactive groups to plant oils is imperative to enhance the reactivity of plant oils, and enables the subsequent introduction of functional groups to the oil [10]. Selecting the appropriate type and number of reactive groups, incorporated within the oil enables its properties, including the glass transition temperature and mechanical characteristics, to be altered to match the desired levels [26, 27].

There are a number of examples that detail the use of the C=C sites in plant oils for chemical modification. For instance, epoxidised plant oils, particularly epoxidised linseed oil (ELO) [14, 26, 28] and epoxidised soy bean oil (ESO) [10, 14], have received considerable attention as bio-based thermosetting

1

resins with the potential to act as alternative materials to petroleum-based products. Various plant oil-based thrermosets were created by reacting ELO or ESO with cyclic anhydride hardeners such as maleic anhydride or phthalic anhydride [3, 28]. ELO and ESO can also be converted into acrylated epoxidised linseed oil (AELO) [5, 28] and acrylated epoxidised soy bean oil (AESO) [10, 26], respectively, by heating with acrylic acid. They are subsequently formulated to make thermosets by using a diluent such as styrene. Norbornene rings and cyclopentadiene rings have also been introduced into soy bean oil to make homogeneous thermosets that are commercially available as Diluin® (Cargill Industrial Specialties) and ML189 (Archer Daniels Midland Company), respectively [29]. Further examples of thermosets made by the modification via the C=C double bond of plant oils include the introduction of hydroxyl [1], carboxyl [13], enone [30], aldehyde [31] and phosphorous-based groups [32].

Herein, we present a method to efficiently convey colour to linseed oil through the conjugation of C. I. Disperse Red 1 (DR1) via the formation of covalent bonds. This enables the uniform dye distribution into the substrate, preventing dye aggregation. DR1 is a commercially available dye that exhibits second-order nonlinear optical (NLO) effect [33] and photo-responsive properties based on light-induced trans-cis isomerisation [34]. The synthesis was accomplished in two straightforward reaction steps. Firstly, thiol-ene click (TEC) reactions are exploited to provide carboxyl (COOH) groups to linseed oil through a reaction with 3-mercaptopropionic acid. This reaction proceeds by following a simple reaction mechanism leading to high product yield, a lack of hindrance by water and oxygen and without the production of undesirable side products [35, 36]. Esterification was then employed to graft DR1 to the functionalised linseed oil, yielding the desired product in a good, highly reproducible, yield. We have proposed the method of producing a thiol-bearing DR1 via chemical modification of DR1, aiming to incorporate the dye into alkene-containing materials by TEC reactions [37]. The method we propose here offers the advantages of simpler reaction procedures and the need for less amount of dye compared to the previous method. It is envisaged that the materials generated are excellent candidates for further employment as precursors to bio-derived coloured coatings.
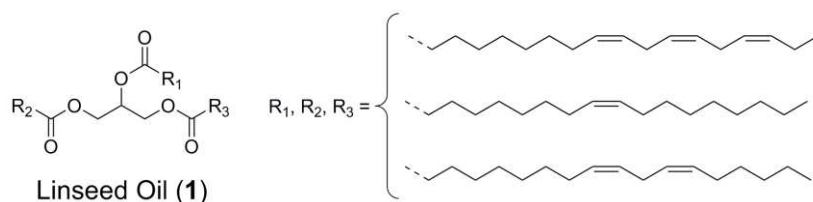
Fig. 1 Chemical structure of Linseed oil (**1**). Three main fatty acid chains are shown here.

2. Experimental
2.1. Materials
Linseed oil, C. I. Disperse Red 1 (dye content 95%), 2, 2′-azobis(2-methylpropionitrile) (AIBN), and 4-(dimethylamino)pyridine (DMAP) were purchased from the Sigma-Aldrich Chemical Company. Dichloromethane (DCM), 3-mercaptopropioic acid and 1-ethyl-3-(3-dimethylaminopropyl)carbodiimide hydrochloride (EDC) were supplied by Alfa Aesar. All the materials were used as received.

2.2 Synthesis
2.2.1 Reaction 1: Synthesis of Modified Linseed Oil (3)

Linseed oil (**1**) was reacted with 3-mercaptopropioic acid (**2**) in order to furnish **1** with pendant COOH units yielding modified linseed oil (**3**) (Scheme 1 Reaction 1). The COOH group enables **1** to readily react with the hydroxyl (OH) group of DR1 by forming an ester bond in the next reaction step. The average molecular weight of **1** was assumed to be 873.60 g/mol based on reported literature value [10]. In order to prevent oxidation, the equipment was purged with nitrogen prior to the reaction. A mixture of **1** (2.62 g, 3.00 mmol), **2** and AIBN (325 mg, 1.98 mmol) was added to a round bottom flask and the mixture was heated with stirring at 80 ℃ under a nitrogen atmosphere for up to 30 hours. DCM (50 mL) was then added to the mixture, and the organic layer was washed with sodium chloride aqueous solution (50 mL) four times, then water (50 mL) twice. Following this, the organic layer was dried over anhydrous sodium sulphide. The product underwent heating at 80 ℃ under reduced pressure for seven hours. A pale yellow clear oil was obtained. The reactions were carried out by varying the amount of **2**, ranging from 0.2 eq. (0.344 mL, 3.95 mmol) to 2.0 eq. (3.45 mL, 39.6 mmol), relative to the number of C=C bonds (6.6 per molecule) in linseed oil [10]. A blank experiment without **2** was also conducted.

2.2.2 Reaction 2: Synthesis of DR1-Conjugated Linseed Oil (5)

The modified linseed oil **3** was then grafted with DR1 (**4**) by esterification [38] to yield DR1-conjugated linseed oil (**5**) (Scheme 1 Reaction 2). 1-ethyl-3-(3-dimethylaminopropyl)carbodiimide (EDC) was used as a condensation reagent and 4-(Ddimethylamino)pyridine (DMAP) was used as a catalyst. The average molecular weight of **3** was assumed to be 1282.26 g/mol as calculated from equation (6) (See Supplementary Information for all equations used in this paper). In a round bottom flask maintained under nitrogen, **3** (256 mg, 0.200 mmol), **4** (194 mg, 0.618 mmol), and DMAP (11 mg, 0.090 mmol) were dissolved in DCM (20 mL). A solution of EDC (295 mg, 1.54 mmol) in DCM (10 mL) was added at room temperature. Stirring at room temperature was then done for varied durations. Following the reaction, washing was performed in the same way as for reaction 1. Following the complete removal of DCM from the organic layer by evaporation, **5** was obtained as a reddish oil. However, unreacted **4** was present as a solid and so the amount of **4** was decreased to the optimal amount (167 mg, 0.532 mmol) (see section 3.2.2), and the same reaction procedure was repeated. The product, **5** was then obtained as a homogeneous reddish oil.

Scheme 1 Synthesis of modified linseed oil (**3**) and DR1-conjugated linseed oil (**5**).

2.3 Characterisation of Modified Linseed Oil (3) and DR1-Conjugated Linseed Oil (5)

^{1}H and ^{13}C NMR spectra were recorded on a Bruker 500 MHz spectrometer using CDCl$_3$ as the solvent and tetramethylsilane (TMS) as the internal standard, and analysed using MestreNova$^®$ Research Lab software. The FT-IR spectra were measured using an ALPHA FT-IR Spectrometer (Bruker Optik GmbH) over a range of 4000 cm^{-1} to 400 cm^{-1}. Mass spectra were measured with a Bruker Maxis Impact mass spectrometer equipped with an electrospray ionisation (ESI) source in positive ion mode over a m/z range of 250 to 3000.

Thermogravimetric analyses (TGA) were undertaken using a TA Instruments TGA Q50 over the temperature range of +30 ℃ to +500 ℃. The measurements were done at a heating rate of +10 ℃/min under a dry nitrogen flow of 40 mL/min for the balance purge flow, and 60 mL/min for the sample purge flow. The onset temperature of the samples was obtained by extrapolating each curve by step transition mode using Universal Analysis 2000 software. Differential scanning calorimetry (DSC) analyses were undertaken using a TA Instruments DSC Q20 over the temperature range of −70 to +200 ℃ at a heating rate of +10 ℃/min under a dry nitrogen flow of 50 mL/min. An empty aluminum pan and lid were used as the reference.

UV-Visible absorption spectra were recorded using a Varian Cary$^®$ 50 UV-Vis spectrophotometer over a range of 210 nm to 800 nm. A blank glass cuvette containing acetonitrile was used as the reference sample.

2.4 Quantification of the Reactions

The quantification of both reactions 1 and 2 were conducted by determining any changes in peak intensities in the relative ^{1}H NMR spectra (See Supplementary Information).

3. RESULTS AND DISCUSSION
3.1 Reaction 1: Synthesis of Modified Linseed Oil (3)
3.1.1 Synthesis

By following the reaction procedure, a pale yellow clear oil was obtained under each reaction condition. The reaction conditions of and the results for reaction 1 are summarised in Table 1.

Table 1 Reaction conditions and calculated conversion ratios in reaction 1.

No.	Molar ratios DB[*1]/**2**/AIBN	Reaction time [hour]	Conversion ratio (X_1)[*2] [%]	No.	Molar ratios DB[*1]/**2**/AIBN	Reaction time [hour]	Conversion ratio (X_1)[*2] [%]
1	1.0/ 2.0/ 0.1	0.5	5.1	25	1.0/ 0.6/ 0.1	0.5	3.8
2	1.0/ 2.0/ 0.1	1	9.2	26	1.0/ 0.6/ 0.1	1	5.9
3	1.0/ 2.0/ 0.1	2	17.8	27	1.0/ 0.6/ 0.1	2	7.1
4	1.0/ 2.0/ 0.1	4	30.0	28	1.0/ 0.6/ 0.1	4	7.8
5	1.0/ 2.0/ 0.1	6	36.5	29	1.0/ 0.6/ 0.1	6	9.4
6	1.0/ 2.0/ 0.1	8	40.1	30	1.0/ 0.6/ 0.1	8	11.8
7	1.0/ 2.0/ 0.1	10	43.3	31	1.0/ 0.6/ 0.1	10	12.8
8	1.0/ 2.0/ 0.1	12	44.9	32	1.0/ 0.6/ 0.1	12	14.1
9	1.0/ 2.0/ 0.1	16	49.6	33	1.0/ 0.6/ 0.1	16	15.0
10	1.0/ 2.0/ 0.1	20	52.3	34	1.0/ 0.6/ 0.1	20	15.8
11	1.0/ 2.0/ 0.1	24	57.6	35	1.0/ 0.6/ 0.1	24	16.2
12	1.0/ 2.0/ 0.1	30	62.0	36	1.0/ 0.6/ 0.1	30	16.4
13	1.0/ 1.0/ 0.1	0.5	8.5	37	1.0/ 0.2/ 0.1	0.5	0
14	1.0/ 1.0/ 0.1	1	7.9	38	1.0/ 0.2/ 0.1	1	0
15	1.0/ 1.0/ 0.1	2	8.5	39	1.0/ 0.2/ 0.1	2	0
16	1.0/ 1.0/ 0.1	4	15.2	40	1.0/ 0.2/ 0.1	4	0.6
17	1.0/ 1.0/ 0.1	6	16.8	41	1.0/ 0.2/ 0.1	6	0.7
18	1.0/ 1.0/ 0.1	8	18.6	42	1.0/ 0.2/ 0.1	8	3.1
19	1.0/ 1.0/ 0.1	10	21.4	43	1.0/ 0.2/ 0.1	10	3.9
20	1.0/ 1.0/ 0.1	12	22.2	44	1.0/ 0.2/ 0.1	12	4.8
21	1.0/ 1.0/ 0.1	16	24.1	45	1.0/ 0.2/ 0.1	16	6.9
22	1.0/ 1.0/ 0.1	20	24.1	46	1.0/ 0.2/ 0.1	20	7.3
23	1.0/ 1.0/ 0.1	24	27.3	47	1.0/ 0.2/ 0.1	24	7.3
24	1.0/ 1.0/ 0.1	30	27.3	48	1.0/ 0.2/ 0.1	30	7.4
				49	1.0/ 0/ 0.1	30	0

[*1] The values represent the amount of C=C bonds (DB) present in **1** before reaction. The average number of C=C bonds in one **1** molecule was assumed to 6.6 [10]. [*2] Calculated from equation (4).

3.1.2 ^{1}H NMR

^{1}H NMR spectra of the starting material **1** and the product **3** (No. 12 obtained in reaction 1 in Table 1) are shown in Fig. 2 (a) and (b), respectively. The ^{1}H NMR spectra produced compare well with spectra obtained in other, related, studies [1, 6, 39, 40, 41].

For **1** [Fig. 2 (a)], the average number of C=C bonds per molecule was calculated to be 6.21 from equation (3) . As the reaction proceeded, the peak from the vinylic proton with cis-C=C configuration at 5.34 ppm (g) decreased. Contrarily, the formation of peaks representative of trans-C=C bonds at 5.40 ppm (g′) were observed.

For **3** [Fig. 2 (b)], the formation of a C-S bond is shown by the presence of the α carbon of the C-S bond protons at 2.58 ppm (k), signifying that the reaction had proceeded. Although this peak was not clear because of the broadening and overlapping of adjacent peaks, the peak was clearly observed on the HQMC chart (See Supplementary Information, Fig. SI 1). Protons present on the β carbons of the C-S bond also appeared at 1.51 ppm (l). The allylic protons adjacent to one C=C bond remained approximately 2.0 ppm (f). The methylene protons derived from **2** were observed around 2.6 ppm (n) and 2.7 ppm (m), respectively. On the other hand, the disappearance of the peak from the allylic protons (h) on the carbon atoms interposed between two C=C bonds were not clear due to the overlapping of peaks from the methylene protons (m). The peak representative of the methyl protons of the linolenic acid chains (18:3) at 0.9–1.0 ppm (i) decreased, whereas the peaks representative of the methyl protons of the other fatty acid chains at 0.8–0.9 ppm (j), increased. This indicates that the C=C bonds on the linolenic acid chains underwent a thiol-ene reaction.

(a)
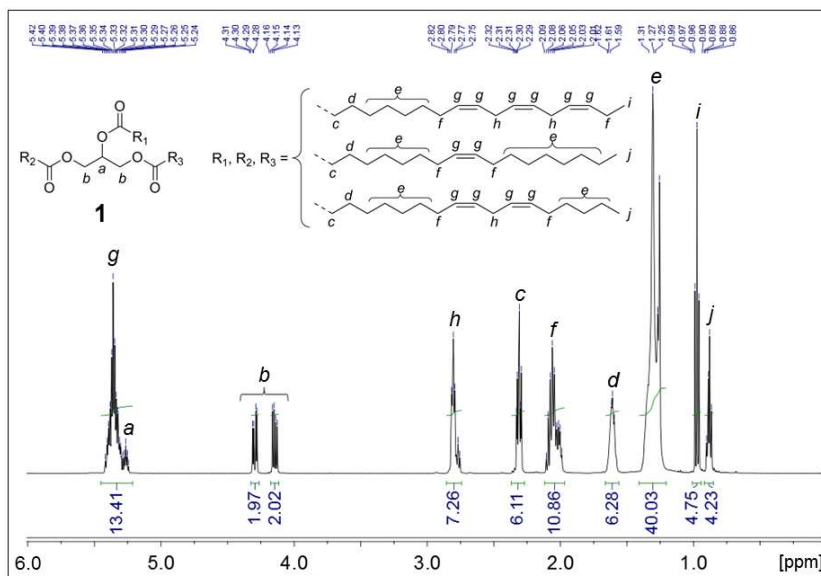
(b)
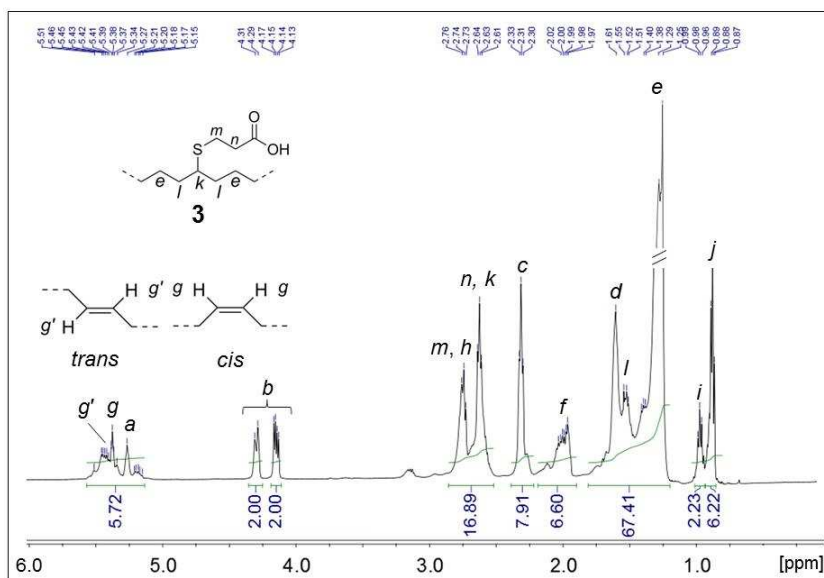
Fig. 2 ^{1}H NMR spectra of (a) **1** and (b) **3** (No. 12 obtained in reaction 1). The chemical structures in (b) show the partial structures of **3** (the bonding between **2** and fatty acid chain, and the C=C bonds).

3.1.3. Quantification of Introduced COOH Units in Modified Linseed Oil (3) under Different Reaction Conditions

Fig. 3 reveals the effect that the amount of **2**, and the reaction time had on the conversion ratios (X_1). When 2.0 eq. of **2** was used (No. 1–12 in reaction 1), the conversion ratio increased with reaction time, finally reaching 62.0% after 30 hours (No. 12), calculated from equation (4) . This value is equivalent to 3.85 units of **2** molecules per one triglyceride molecule, calculated from equation (5). When the amount of **2** was changed to 1.0 eq. (No. 13–24), 0.6 eq. (No. 25–36) or 0.2 eq. (No. 37–48), similar behaviour was observed. However, the resulting conversion ratios after 30 hours were 27.3% (No. 24), 16.4% (No. 36), and 7.4% (No. 48), respectively, which were less than the value obtained in No. 12. The reason why the high concentration of **2** yielded high conversions is explained by the fact that thiole-ene reaction involves a rate-determining step where carbon radicals abstract a hydrogen from a thiol compound such as **2** [41]. Higher concentrations of **2** more effectively trap the carbon radicals [40]. In all the experiments performed, washing was required to remove any remaining **2** following the reactions. As a result, using 2.0 eq. of **2** was considered to be optimal for high product yield and minimal removal of unreacted **2**. When a blank experiment was undertaken without **2** (No. 49), no conversion was observed, signifying that ene-ene homocoupling or oxidative reactions did not take place under the reaction conditions of No. 49.
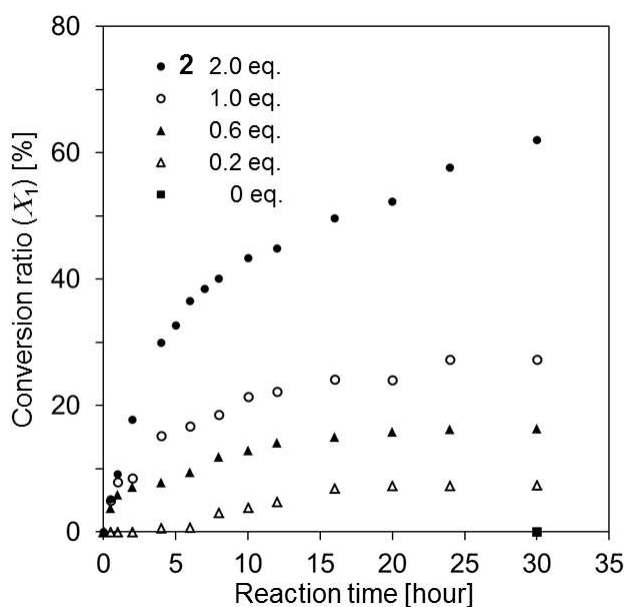
Fig. 3 The effect of the amount of **2** and the reaction time on the conversion ratios (X_1).

3.1.4. FT-IR

FT-IR results of the starting material **1** and the product **3**, produced by using 2.0 eq. of **2** at different reaction times are shown in Fig. 4 [20, 40].

In **1**, peaks corresponding to the cis-C=C bonds [cis-(C-H)=CH stretching: 3010 cm^{-1}, cis-(C=C) stretching: 1658 cm^{-1})] and triglyceride esters (C=O stretching: 1738 cm^{-1}) were observed.

In **3**, these cis-C=C peaks decreased upon conversion according to the reaction, disappearing completely in 30 hours (No. 12). Another peak of cis-C=C bonds [cis-(C-H)=CH wagging: 721 cm^{-1}] decreased due to the reaction, but it is not certain that this peak disappeared completely or not, because of the existence of a (CH$_2$)$_n$ rocking peak at the same region. On the other hand, an isolated trans-C=C bond [967 cm^{-1}: trans-(C-H)=CH wagging] was formed. In the thiol-ene reaction, the addition of the thiyl radical, which is generated during the reaction, to C=C bonds proceeds reversibly, and the thiyl radical isomerises cis-C=C bonds to trans-C=C bonds, because trans formation is more thermodynamically stable than cis formation [41]. In No.12, peaks representing the trans-C=C bonds were still observed, signifying incomplete conversion. As **1** contains fatty acid chains with more than one C=C bond, such as the linolenic acid chain (18:3), it may be suggested that the steric effect of the additional side chain made the C=C bonds less susceptible to thiyl attack and subsequent hydrogen abstraction, and thus prevented the quantitative conversion of C=C bonds [1, 39]. In contrast, quantitative conversation may be predicted for the fatty acid chain which includes one C=C bond, such as the oleic acid chain (18:1), within its structure [1, 39].

COOH groups derived from **2** were also observed in all the products of **3** obtained [OH stretching: 2500–3500 cm^{-1}, C=O stretching: 1711 cm^{-1}, (C-C-O) asymmetric stretching: 1241 cm^{-1}, (C-O) stretching: 1159 cm^{-1}, (O-CH$_2$-C) asymmetric stretching: 1100 cm^{-1}]. Those peaks increased with reaction time, before reaching a plateau, as clearly demonstrated by the C=O stretching band at 1711 cm^{-1}. In addition to CH$_2$ bending of **1** at 1458 cm^{-1}, other **2**-derived CH$_2$ bending peaks were observed at 1434 cm^{-1} and 1414 cm^{-1}. The absence of a thiol peak from **2** (SH stretching: 2567 cm^{-1}) indicated that **2** was almost removed by treatment following the reaction. As in **1**, other CH peaks were observed in **3** such as the asymmetric stretching of CH$_3$ at 2960 cm^{-1}, and of CH$_2$ at 2923 cm^{-1}, and the symmetric stretching of CH$_2$ at 2853 cm^{-1}.
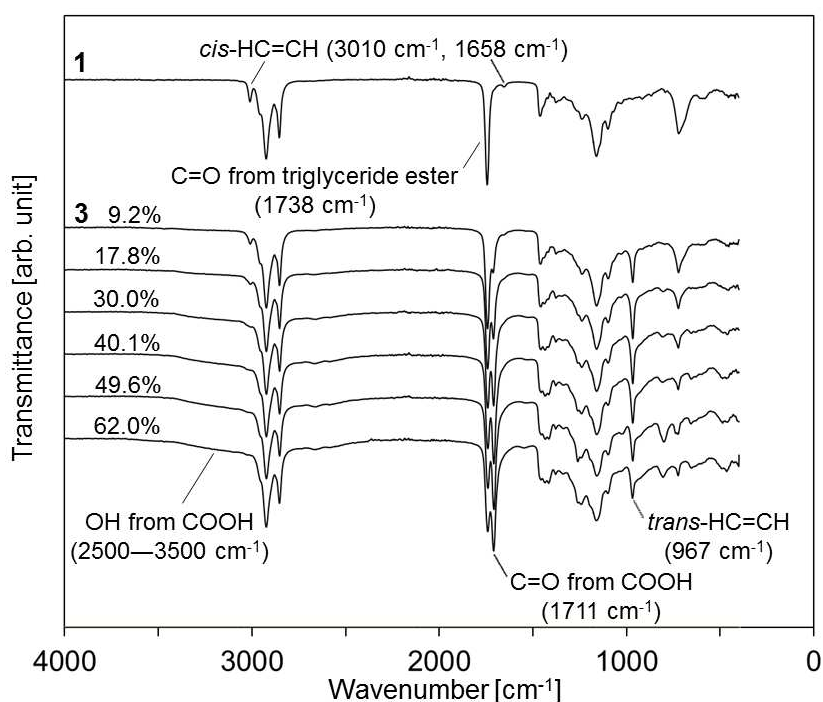
Fig. 4 FT-IR spectra of **1** and **3** obtained with different conversion ratios [9.2% (No. 2), 17.8% (No. 3), 30.0% (No. 4), 40.1% (No. 6), 49.6% (No. 9), 62.0% (No. 12) obtained in reaction 1].

3.1.5. ^{13}C NMR

^{13}C NMR analysis also confirmed that **2** successfully reacted with the C=C bonds of **1**. Assignments were compared to the literature [1, 39, 40, 41, 42] and HMQC results (See Supplementary Information, Fig SI 1). The ^{13}C NMR spectra of **1** and **3** (No. 12 obtained in reaction 1) are shown in Fig. 5 and Fig. 6, respectively.

For **1** (Fig.5), strong peaks corresponding to the C=C bonds at 129–132 ppm (8) are characteristic of plant oils. Linseed oil **3** has a high concentration of fatty acid chains derived from linolenic acid chain (18:3) as observed at 20.5 ppm (10). Also, methyl carbons derived from linolenic acid chain (18:3), oleic acid chain (18:1), and linoleic acid chain (18:2) were observed at 13.9–14.2 ppm (11).

For **3** (Fig. 6), a decrease in the intensity of the peak representative of the C=C bonds (8) was observed. Additionally, the allylic carbon peaks adjacent to one C=C bond at 27.1–27.2 ppm (7), and located between two C=C bonds at 25.4–25.6 ppm (9) decreased significantly. On the other hand, peaks corresponding to the carbon atoms that are part of the newly formed C-S bond at α, β, γ positions, adjacent to the sulphur atom, were observed at 46.3 ppm (14), 34.9 ppm (15) and 26.6–26.8 ppm (16), respectively, signifying the formation of a C-S bond. Also, two different methylene carbons and the carboxylic carbon from **2** units were observed at 24.9–25.2 ppm (17), 34.8–35.1 ppm (18), and 178.0 ppm (19) respectively. No peaks representative of residual **2** (19 ppm and 39 ppm) were observed.

(a)
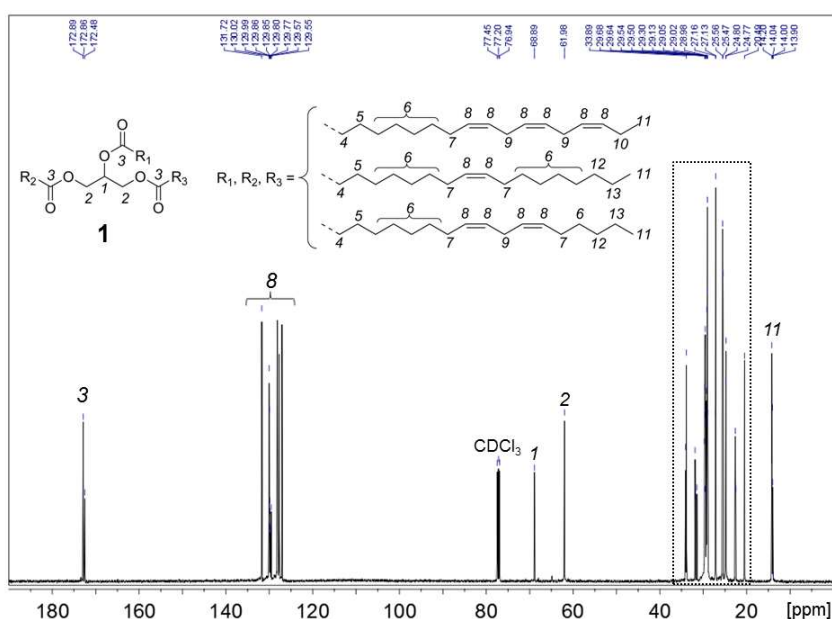
(b)
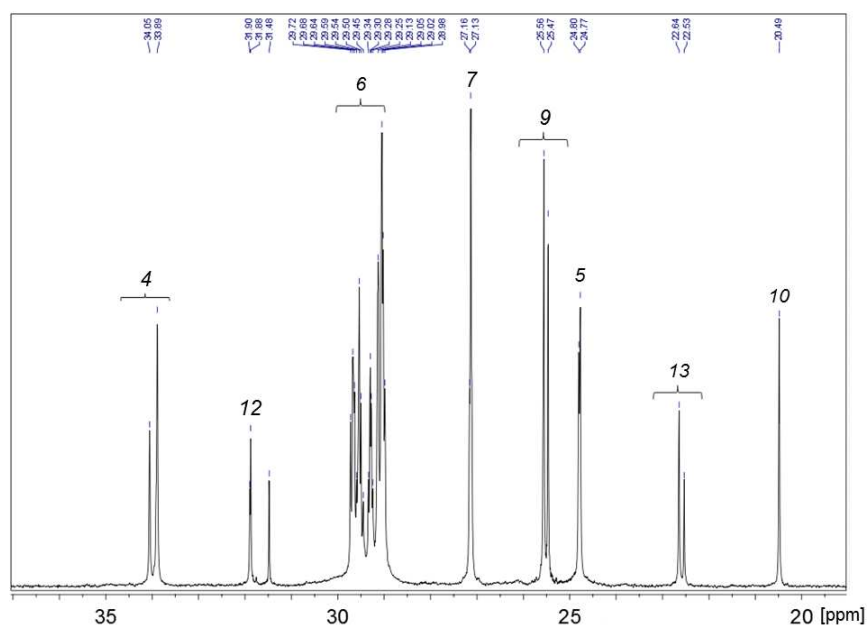
Fig. 5 ^{13}C NMR spectra of **1**: (a) The range of 0–190 ppm, (b) A magnified view of the range of 19–37 ppm.

10

(a)
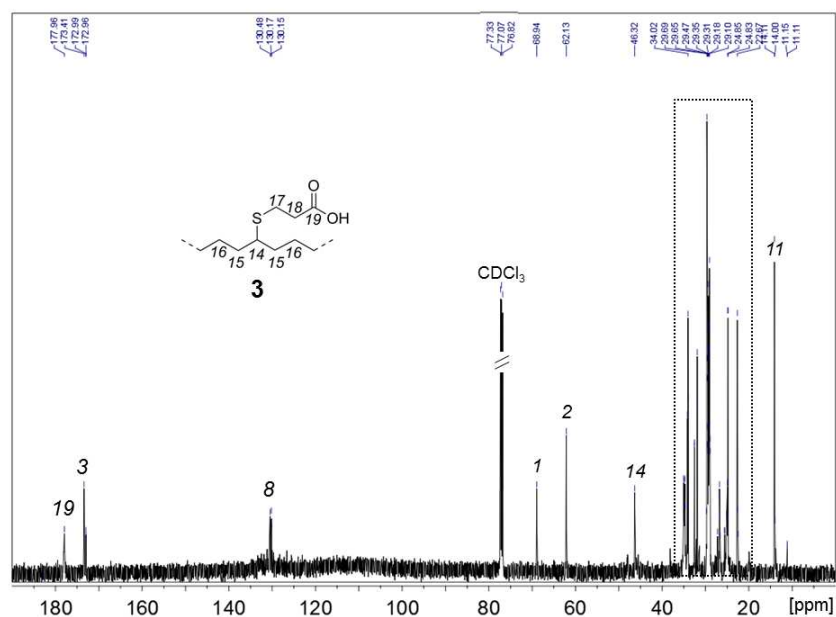
(b)
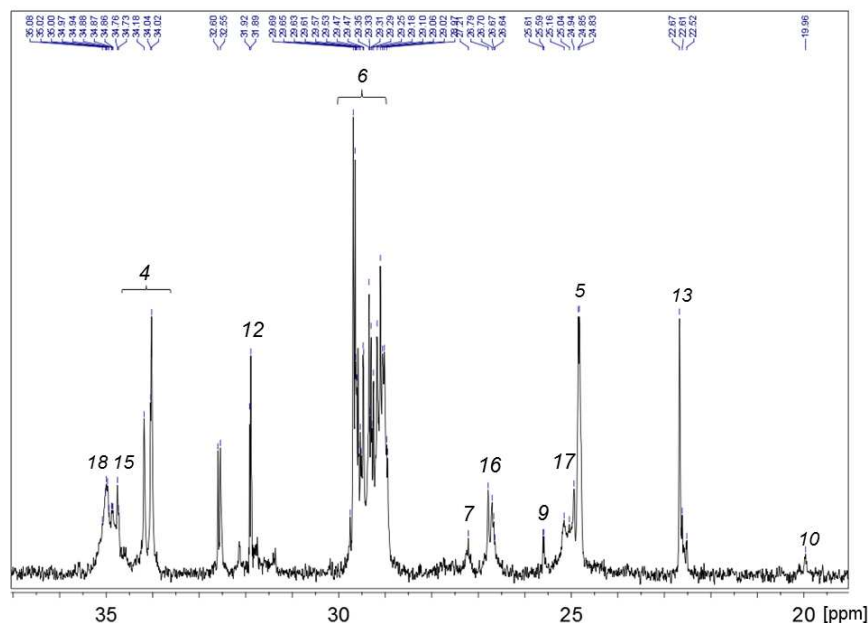
Fig. 6 ^{13}C NMR spectra of **3** (No. 12 obtained in reaction 1): (a) The range of 0–190 ppm, (b) A magnified view of the range of 19–37 ppm. The chemical structure in (a) shows a partial structure of **3** (the bonding between **2** and fatty acid chain). Peaks 1–13 derive from the chemical structure shown in Fig. 5 (a).

3.2 Reaction 2: Synthesis of DR1-Conjugated linseed oil (5)
3.2.1 Synthesis

Modified linseed oil **3** (No. 12 obtained in reaction 1) was utilised to afford coloured linseed oil. In experiment No.1, 0.80 eq. of **4** relative to the amount of COOH groups available in **3** (calculated using equation (6)) were used. During the reaction, the TLC spot of **4** became weaker but it did not disappear following five hours of reaction. The reaction was continued for up to 24 hours, but no clear change was observed by TLC. Upon reaction completion, a mixture of reddish oil and reddish solid were obtained, and the solid was confirmed by ^{1}H NMR to be unreacted **4**. In experiment No.2, the initial amount of **4** was decreased so that the molar concentration of **4** equalled the molar concentration of available COOH sites present on **3.** The required concentrations of **3** and **4** were calculated using ^{1}H NMR, as described in 3.2.2. In this case, a homogeneous reddish oil was obtained exclusively, signifying an optimised reaction. The

11

reaction conditions and the results for reaction 2 are summarised in Table 2.

3.2.2. ^{1}H NMR

^{1}H NMR spectra of the obtained compounds (No. 1 and No. 2 in reaction 2 in Table 2) are shown in Fig. 7 (a) and (b), respectively. In reaction No.1 [Fig. 7 (a)], the methylene protons in proximity to the OH group, which appeared at 3.88–3.90 ppm (o), 3.3.61–3.63 ppm (p), and 3.56–3.59 ppm (q) of **4**, were shifted to 4.27–4.32 ppm (o′), 3.68 ppm (p′), and 3.53 ppm (q′), respectively, due to the esterification between the OH group of **4** and the COOH group of **3**. Unreacted **4** was quantified by comparing the remaining isolated o peak with peaks corresponding to the aromatic protons of **4** unit observed at 8.3 ppm (v), 7.9 ppm (t and u), and 6.8 ppm (s), and was found to be 0.11 eq. compared to the COOH amount, which was calculated from equation (5). Thus, in No. 2, the amount of **4** was decreased to 0.69 (= 0.80 − 0.11) eq. in order to consume all of **4** in the reaction. The ^{1}H NMR results in No. 2 [Fig. 7 (b)] show the disappearance of o peak, signifying the complete consumption of **4** by the esterification. This change suggests that the product obtained in No. 2 was the desired product **5**. Other distinct peaks were similar to peaks in **3**, and displayed negligible change during the reaction.

(a)

(b)
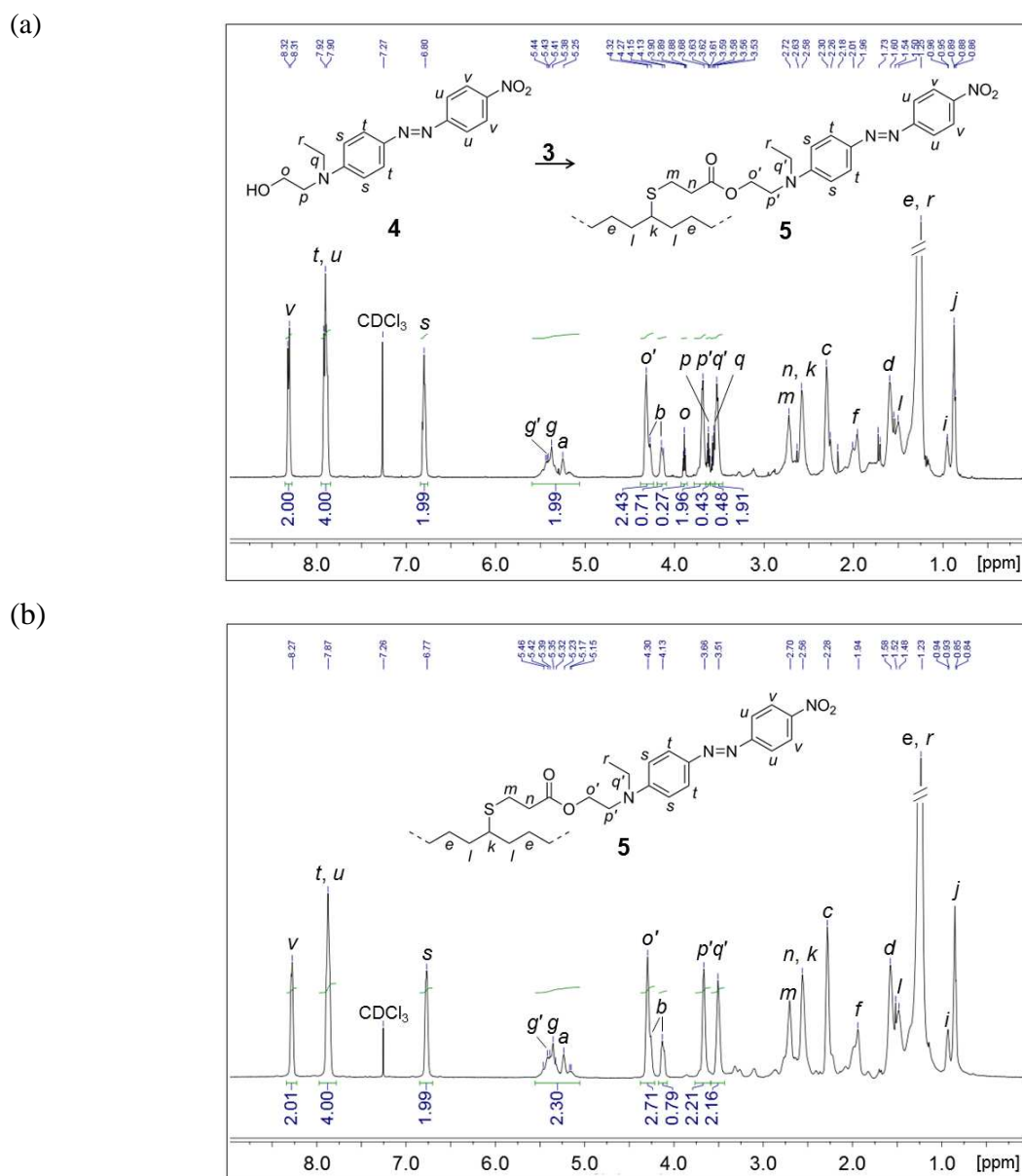
Fig. 7 ^{1}H NMR spectra of the compounds obtained from reaction 2; different amounts of **4** were used: (a) 0.80eq. (No. 1), (b) 0.69 eq. (No. 2) relative to the amount of COOH groups available in **3**. Chemical structures show the partial structure of **5** (the bonding between **4** and fatty acid chain). Peaks a–j are derived from the chemical structure shown in Fig. 2.

12

Table 2. Reaction conditions and results in reaction 2

No.	Molar ratios COOH[*1]/**4**/EDC/DMAP	Reaction time [hour]	Products	Conversion ratios[*2]	
				X_2 [%]	$X_{overall}$ [%]
1	1.0/0.80/2.0/0.01	24	**5** and unreacted **4**	63.1	39.1
2	1.0/0.69/2.0/0.01	5	**5**	63.1	39.1

[*1] The values represent the amount of COOH groups present in **3** before reaction. The average number of COOH groups in one **3** molecule was assumed to 3.85 as calculated from equation (5). [*2] Calculated from equation (8) for X_2 and (9) for $X_{overall}$.

3.2.3. Quantification of Conjugated DR1 in DR1-Conjugated Linseed Oil (5)

The quantification of the mean extent to which **4** was conjugated to one molecule of **3** to yield **5** was accomplished using equation (9). It was found that 2.43 molecules of **4** were conjugated to each molecule on average in both No. 1 and No. 2. The number is equal to 39.1% of the C=C bonds present in linseed oil ($X_{overall}$). The correspondence of both figures shows that all of the presumably reactive COOH units of **3** conjugated to **4**. The results indicate that the amount of conjugated **4** was less than the number of COOH units (3.85), and 63.1% of COOH units in **3** were used for DR1 conjugation (X_2), signifying the possibility that some C=C bonds in **3** participated in side reactions such as ene-ene homocoupling [43] during reaction 1, and/or some COOH units on **3** were not reactive towards **4** during reaction 2.

3.2.4. ^{13}C NMR

The ^{13}C NMR spectra of **5** are shown in Fig. 8 The shift of the peak that is representative of the carboxylic carbon in **3** from 178 ppm (19) to 172 ppm (19′) suggests the formation of an ester bond. A peak representative of EDC was not observed in any experiment conducted.

(a)
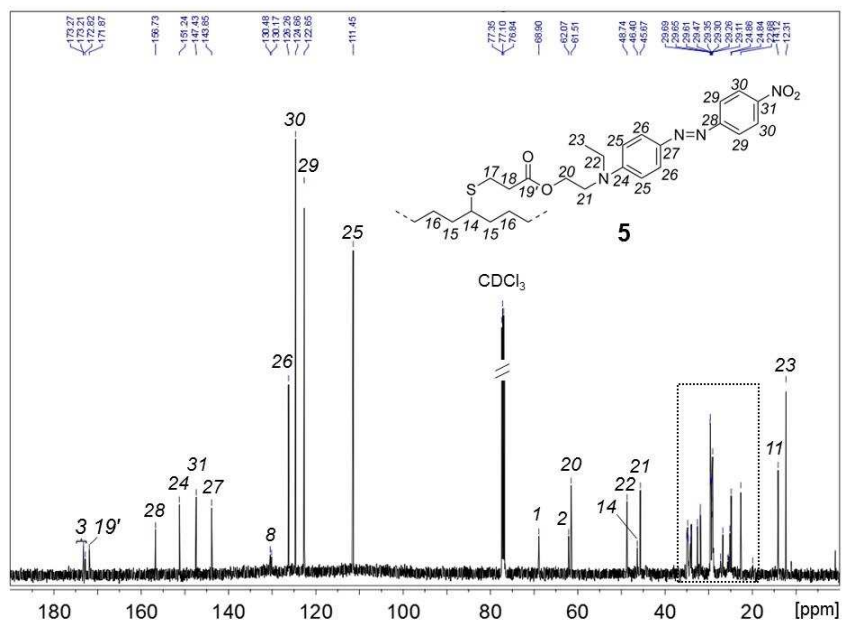
(b)
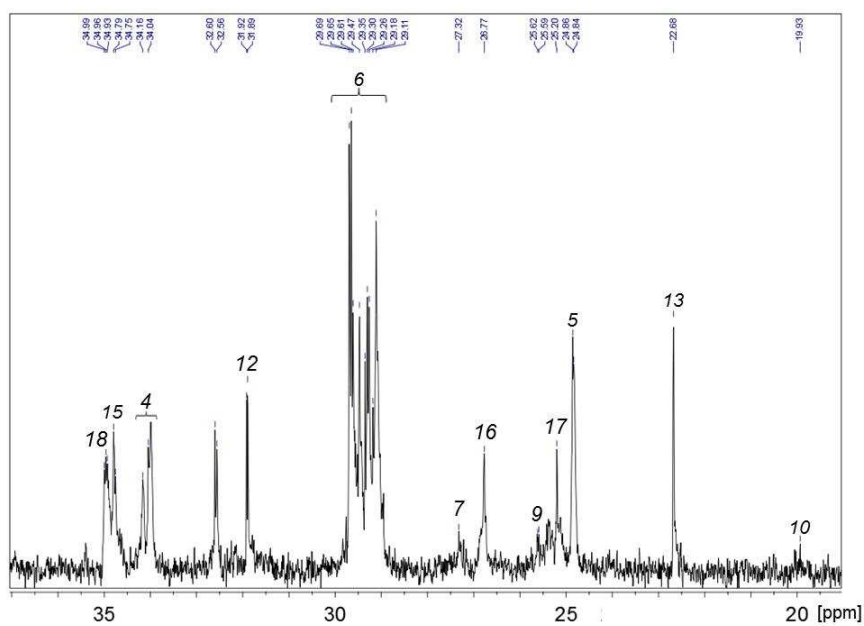
Fig. 8 ^{13}C NMR spectra of **5** (No. 2 obtained in reaction 2): (a) The range of 0–190 ppm, (b) A magnified view of the range of 19–37 ppm. The assignments were done by HMQC and HMBC results, and reported theoretical values [44]. Peaks 1–13 derive from the chemical structure shown in Fig. 5 (a) and Fig. 6 (a).

3.2.5. FT-IR

The FT-IR spectra of the dye coupling reactants [**3** (No. 12 obtained in reaction 1) and **4**], and the obtained products in reaction 2 (No. 1 and No. 2) are provided in Fig. 9 [44]. The FT-IR spectrum corresponding to the product (No. 2) showed the large decrease of both the OH group of **4** (3100–3500 cm^{-1}) and the COOH group of **3** (OH stretching: 2500–3500 cm^{-1}, C=O stretching: 1711 cm^{-1}). These changes suggested the consumption of **3** and **4**, and the successful formation of an ester bond between them. In the product of No. 1, however, a weak OH peak was observed, which indicated the existence of unreacted **4** due to an excess of **4** used. Other peaks derived from **4** units were observed in **5** which are from NO_2 (asymmetric stretching: 1515 cm^{-1}, symmetric stretching: 1336 cm^{-1}, scissoring: 858 cm^{-1}, C-NO_2 stretching: 1104 cm^{-1}), C-N (stretching: 1387 cm^{-1}), phenylene (C=C-C stretching: 1600 cm^{-1}, 1515 cm^{-1}, and 1131 cm^{-1}, out-of-plane bending of CH: 858 cm^{-1}, in-plane bending of CH: 1131 cm^{-1}), CH_2 (wagging and twisting : 1387 cm^{-1}), and CH_3 (wagging: 1387 cm^{-1}). No peak corresponding to EDC was observed.
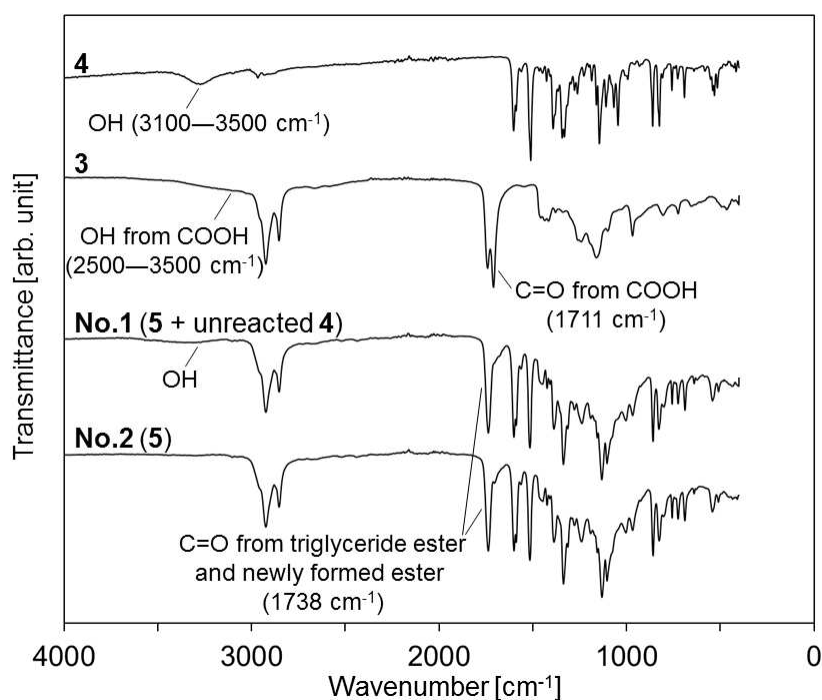
Fig. 9 FT-IR spectra of reactants [**3** (No. 12 obtained in reaction 1) and **4**] and obtained products [No.1 and No. 2 (**5**) obtained in reaction 2].

3.2.6. Mass-spectrometry

The results of mass spectrometry also supported the characterisations. Fig 10 shows the ESI mass spectra of (a) **1**, (b) **3** (No. 12 obtained in reaction 1), and (c) **5** (No. 2 obtained in reaction2)

The spectrum corresponding to **1** [Fig. 10 (a)] reveals multiple peaks due to the existence of various fatty acid chains and their different adducts, including hydrogen adducts ($[M + H]^+$) and sodium adducts ($[M + Na]^+$). Strong peaks at m/z = 890–914 derive from triglyceride molecules with different number of C=C bonds.

The spectrum corresponding to **3** [Fig. 10 (b)] reveals that the strong peaks observed in **1** decreased, while several main peaks were observed. The peak at m/z = 1216.81 was considered to derive from the sodium adduct of triglyceride molecule **3** which has four C=C bonds and three COOH groups (#DB/#COOH = 4/3) in its three fatty acid chains which consist of 18 carbon atoms per chain. The difference between the observed value and theoretical value (m/z = 1217.74) might be due to one hydrogen abstraction occurring during measurements and/or weak intensities. Around each strong peak, several peaks were also observed. Around at m/z = 1216.81, for instance, peaks were observed at m/z = 1214.79 and 1218.82. These values differ from 1216.81 by approximately 2.02, signifying the difference of these three molecules comes from the difference in the number of C=C bonds among them. These strong peaks had the interval of m/z = 106.01 or 106.01 ± 2.02. The interval of m/z = 106.01 is equivalent to an increase in mass that equates to a single **2** molecule being attached to one **1** molecule. Accordingly, the synthesised **3** was considered to have one–six COOH groups. These results supported the calculated conversion ratio of X_1. The absence of higher species above m/z = 1700 signified that homo-homo coupling hardly occurred during reaction 1.

The spectrum corresponding to **5** [Fig. 10 (c)] reveals strong peaks starting from around m/z = 1114.91, separated by the regular interval of m/z = 400.12. This interval is equivalent to an increase in mass that equates to one hydrogen on a methylene chain in **3** being substituted with one **4**-conjugated unit [as shown in the chemical structure in Fig. 10 (c)]. The strong peak, for example at m/z = 1515.03 was considered be from the molecule which has unreacted both three C=C bonds and two COOH groups, and one conjugated **4** (#DB/#COOH/#conjugated **4** = 3/2/1; theoretical value of m/z = 1515.88). Around the peak other peaks such as m/z = 1517.04 (2/2/1), 1513.22 (4/2/1) were observed. The results also supported the calculated conversion ratio of X_2.

(a)

(b)

(c)
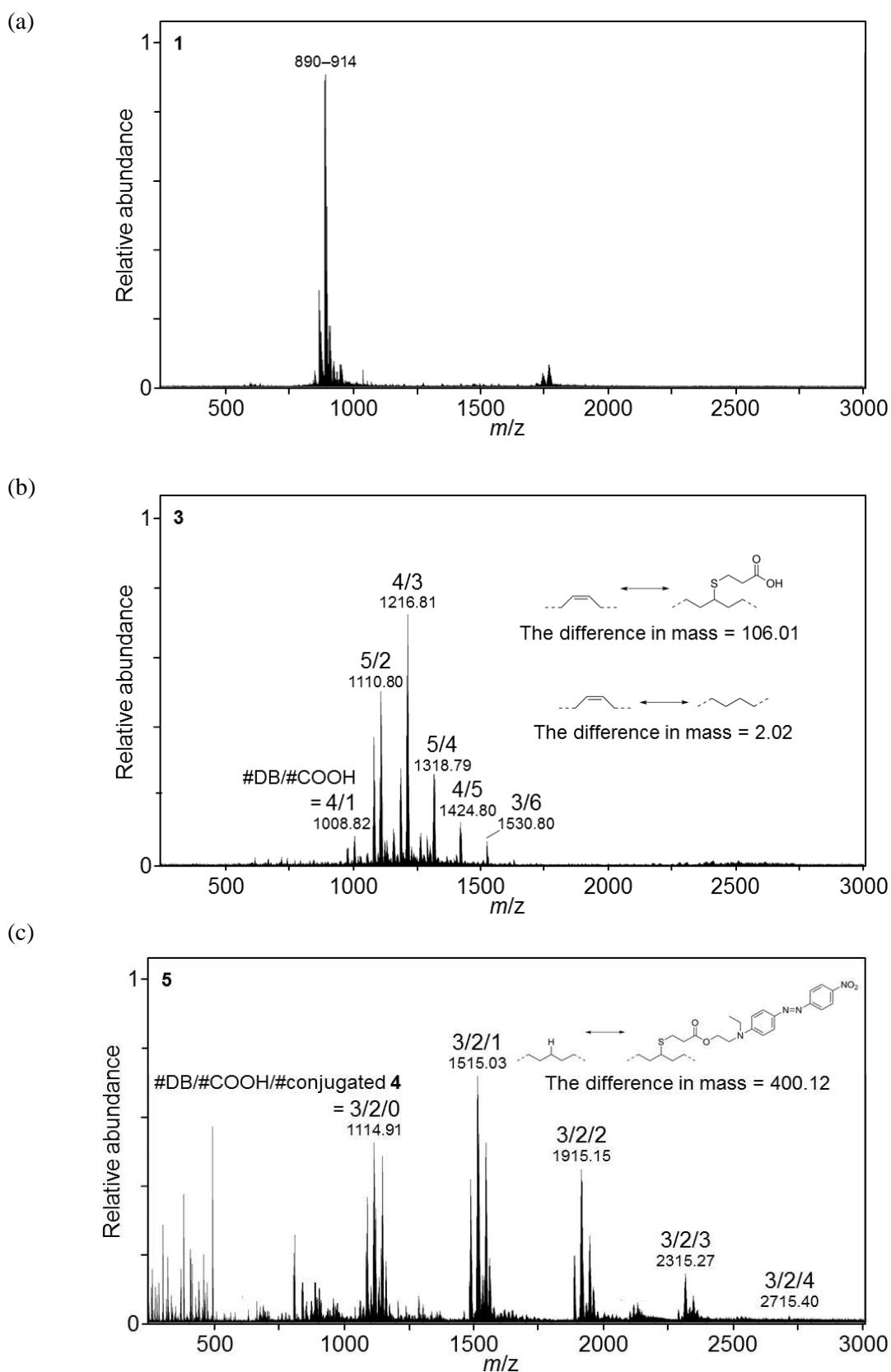
Fig. 10 ESI (positive) mass spectra of (a) **1**, (b) **3** (No. 12 obtained in reaction 1), and (c) **5** (No. 2 obtained in reaction2) in the range of m/z = 250–3000. Figures written at the top of each group of peaks means the observed main peaks with the estimated number of following structures per molecule: C=C double bonds (#DB), COOH groups (#COOH) which derive from bonded **2**, and the number of **4** conjugated to the COOH group on **3** (# conjugated **4**).

17

4. Thermal Properties and UV-Vis Spectroscopic Properties

Thermal analyses and UV-Vis spectroscopic analyses were conducted on the starting materials and the products formed. The results are summarised in Table 3.

Table 3. Thermal properties and UV-Vis spectroscopic properties of various compounds.

Samples	TGA	DSC		λ_{max} [nm]
	T_d [°C]	T_m [°C]	T_p [°C]	
Linseed Oil (**1**)	368.7	−25.9	-	-
Modified Linseed Oil (**3**)[*1]	286.6	−3.90	−27.9	-
DR1 (**4**)	263.1	165.2	-	487
DR1-Congugated Linseed Oil (**5**)[*2]	223.6, 328.3	41.2	-	476

T_d: thermal decomposition temperature, T_m: melting temperature, T_p: phase transition temperature, λ_{max}: maximum absorption wavelength. [*1] No. 12 obtained in reaction 1 and [*2] No. 2 obtained in reaction 2.

4.1. Thermal Properties
4.1.1. TGA

Fig. 11 shows the TGA curves of samples **1**, **3** (No. 12 obtained in reaction 1), **4**, and **5** (No. 2 obtained in reaction 2). A decrease in the mass due to thermal decomposition of the samples was observed upon heating all of the samples. Linseed oil, **1** showed the onset of thermal decomposition temperature (T_d) at 368.7 ℃. For modified linseed oil **3**, the onset of decomposition temperature was 286.6 ℃. The data obtained indicates that a higher conversion ratio results in a lower T_d of **3** (See Supplementary Information, Fig. SI 2). The dye, **4**, showed an T_d of 263.1 ℃. The final product **5** showed two decomposition points that originated at 223.6 ℃ and 328.3 ℃ and corresponded to the decomposition of **3** and **4**, respectively.
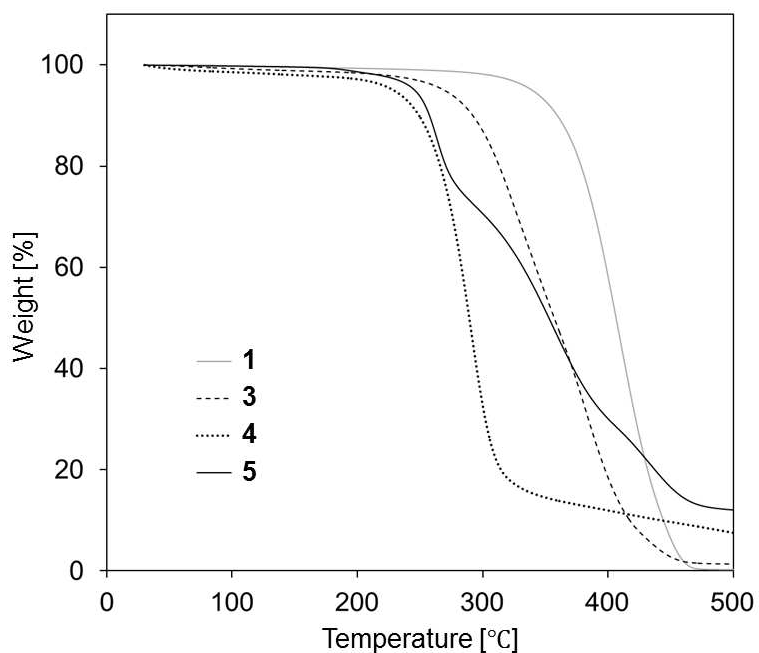
Fig. 11 TGA curves of **1**, **3** (No. 12 obtained in reaction 1), **4**, and **5** (No. 2 obtained in reaction 2).

4.1.2. DSC

Fig. 12 shows the DSC thermograms of the same samples used for the TGA measurements. **1** showed an endothermic peak corresponding to the melting temperature (T_m) at −25.9 ℃, and an exothermic peak at 140.8 ℃. The latter peak is from the formation of hydroporoxides which are primary products of the oxidation of **1** [45, 46]**,** caused by its reaction with dissolved oxygen. Samples **3** and **5** did not show the corresponding peak suggesting that their drying properties are lower than that of **1**, because of the decrease in the number of C=C bonds due to the bonding with **2**.

The modified oil **3** also showed a T_m at −3.90 ℃. Additionally, **3** revealed an exothermic peak at −27.9 ℃ which might reflect a phase transition at the lower temperature region. The data obtained indicates that a higher conversion ratio correlates to a higher T_m and a higher phase transition temperature (T_p) for **3** (See Supplementary Information, Fig. SI 3). Interestingly, **5** did not show the endothermic peak at 165.2 ℃, which is the T_m of **4**, but showed a different endothermic peak at 41.2 ℃, due to the material melting.
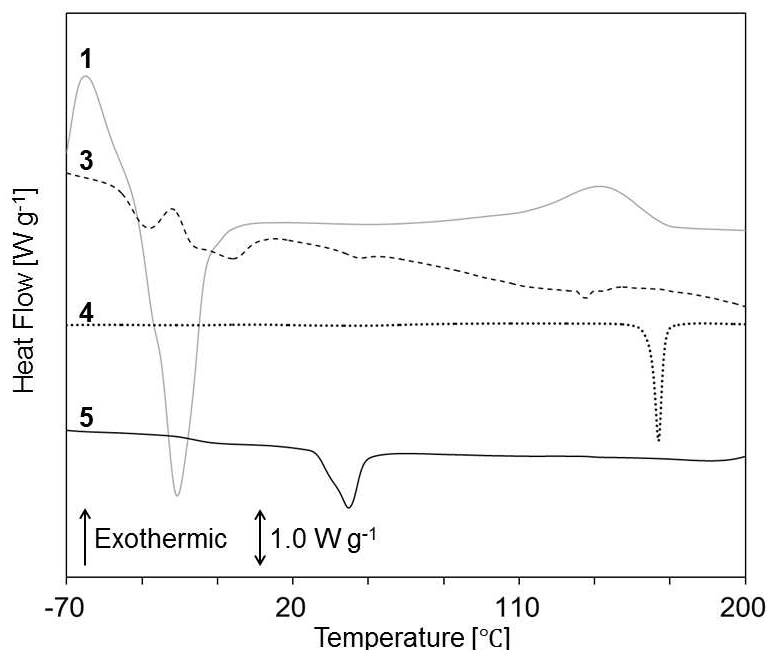
Fig. 12 DSC curves of **1**, **3** (No. 12 obtained in reaction 1), **4**, and **5** (No. 2 obtained in reaction 2).

4.2. UV-Vis spectroscopic properties

The UV-visible spectra of **3** (No. 12 obtained in reaction 1), **4**, and **5** (No. 2 obtained in reaction 2) in acetonitrile are shown in Fig. 13. The modified linseed oil **3** showed minimal absorption in this region. The dye **4** had a maximum absorption wavelength (λ_{max}) at 487 nm, while **5** had a λ_{max} at 476 nm. The hypsochromic shift of 11 nm in **4** following the chemical modification signified the successful conjugation of **3** and **4** [37, 47]. This shift was not caused by solvatochromism, a mixture of **1** and **4** (with the same concentrations as **5**) produced a similar spectroscopic curve (λ_{max} = 488 nm) to that of **4**. This hypsochromic shift may be explained by the introduction of the chemical bond (-O-C=O) which bond decreases the electron-donating ability of the donor unit, resulting in a decrease in the HOMO level of **5**.
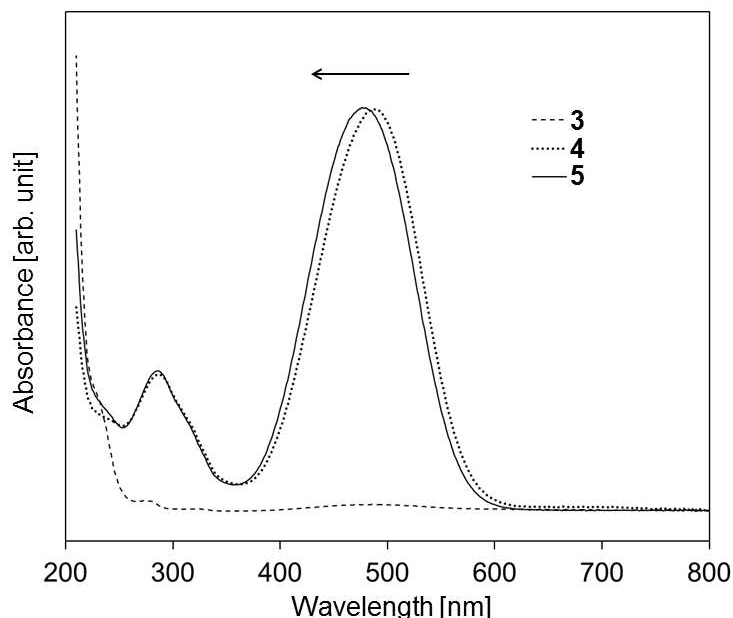
Fig. 13 UV-visible absorption spectra of **3** (No. 12 obtained in reaction 1), **4** and **5** (No. 2 obtained in reaction 2).

5. CONCLUSION

DR1-conjugated linseed oil was synthesised by conjugating DR1 to linseed oil in two chemically-straightforward coupling steps. The formation of DR1-conjugated linseed oil was verified by ^{1}H, ^{13}C NMR , FT-IR and mass spectrometry. Linseed oil was initially reacted with 3-mercaptopropioic acid via a highly-effective thiol-ene reaction to introduce COOH functionality to the oil. By varying the amount of 3-mercaptopropionic acid and the reaction time, the extent of COOH functionality on the modified oil was controlled. Using ^{1}H NMR it was calculated that a maximum of 62.0% of the C=C bonds available were modified. The incorporated COOH units then underwent esterification with DR1 to form a covalent bond between the modified oil molecules and the dye molecules. In total, 39.1% of the initial C=C bonds available in linseed oil were conjugated with DR1 on average. Thermal analyses revealed that the product has two decomposition temperatures at 223.6 ℃ due to DR1, and at 328.3 ℃ due to linseed oil. Moreover, the product expressed a melting temperature at 41.2 ℃ which is approximately 120 °C lower than that of DR1. UV-Vis spectroscopy revealed a maximum absorption of the product at 476 nm, and a 11 nm hypsochromic shift from DR1. These features signified the formation of a covalent bond between modified linseed oil and DR1, formed in a chemically simplistic manner. It is anticipated that this method of oil-dye conjugation, which enables the extent of dye conjugation to be readily controlled, may be exploited for the creation of coloured, bio-derived, molecules that possess the desired properties to be applied as coatings.

21

6. References

[1] Desroches M.; Caillol S.; Lapinte V.; Auvergne R.; Boutevin B. Synthesis of Biobased Polyols by Thiol Ene Coupling from Vegetable Oils. Macromolecules 2011; 44: 2489–2500.

[2] Motawie A. M.; Hassan E. A.; Manieh A. A.; Aboul-Fetouh M. E.; Fakhr El-Din A. Some Epoxidized Polyurethane and Polyester Resins Based on Linseed Oil. J. Appl. Polym. Sci. 1995; 55: 1725–32.

[3] Rösch J.; Mülhaupt R. Polymers from renewable resoureces: polyester resins and blends based upon anhydride-cured epoxidized soybean oil. polym bulletin 1993; 31: 679–86.

[4] Alam M., Akram D., Sharmin E., Zafar F., Ahmad S. Vegetable oil based eco-friendly coating materials: A review article. Arabian J. Chem. 2014; 7: 469–79.

[5] Wuzella G.; Mahendran A. R.; Müller U., Kandelbauer A.; Teischinger A. Photocrosslinking of an Acrylated Epoxidized Linseed Oil: Kinetics and its Application for Optimized Wood Coatings. J. Polym. Environ. 2012; 20: 1063–74.

[6] Zovi O.; Lecamp L.; Loutelier-Bourhis C.; Langeb C. M.; Bunela C. A solventless synthesis process of new UV-curable materials based on linseed oil. Green Chem. 2011; 13: 1014–22.

[7] Alam M., Ray A. R.; Ashraf S. M.; Ahmad S. Synthesis, Characterization and Performance of Amine Modified Linseed Oil Fatty Amide Coatings. J. Am. Oil Chem. Soc. 2009; 86: 573–80.

[8] Black M.; Rawlins J. W. Thiol–ene UV-curable coatings using vegetable oil macromonomers. Eur. Polym. J. 2009; 45: 1433–41.

[9] La Scala J.; Wool R. P. Rheology of Chemically Modified Triglycerides. J. Appl. Polym. Sci. 2005; 95: 774–83.

[10] Khot S. N.; Lascala J. J.; Cane., Morye S. S.; Williams G. I.; Palmese G. R.; Kusefoglu S. H., et al. Development and Application of Triglyceride-Based Polymers and Composites. J. Appl. Polym. Sci. 2001; 82: 703–23.

[11] R. P. Wool US Patent 6 121 398 2000.

[12] Ding C.; Matharu. A. S. Recent Developments on Biobased Curing Agents: A Review of Their Preparation and Use. ACS Sustainable Chem. Eng. 2014; 2: 2217−36.

[13] Jaillet F.; Desroches M.; Auvergne R.; Boutevin B.; Caillol S. New biobased carboxylic acid hardeners for epoxy resins. Eur. J. Lipid Sci. Technol. 2013; 115: 698–708.

[14] Muturi P.; Wang D.; Dirlikov S. Epoxidized vegetable oils as reactive diluents I. Comparison of vernonia, epoxidized soybean and epoxidized linseed oils. Prog. Org. Coat. 1994; 25: 85–94.

[15] Schneider M. P. Review Plant-oil-based lubricants and hydraulic fluids. J. Sci. Food Agric. 2006; 86: 1769–80.

[16] Willing A. Lubricants based on renewable resources — an environmentally compatible alternative to mineral oil products. Chemosphere 2001; 43: 89–98.

[17] Force C. G.; Starr F. S. Vegetable oil adducts as emollients in skin and hair care products. US Patent, 4,740,367, 1988.

[18] Meier M. A. R.; Metzgerb J. O.; Schubert U. S. Plant oil renewable resources as green alternatives in polymer science. Chem. Soc. Rev. 2007; 36: 1788–802.

[19] Mallégol J.; Lemaire J.; Gardette J. L. Drier influence on the curing of linseed oil. Prog. Org. Coat. 2000; 39: 107–13.

[20] Lazzari M.; Chiantore O. Drying and oxidative degradation of linseed oil. Polym. Degrad. Stab. 1999; 65: 303–13

[21] Ronda J. C.; Lligadas G.; Galià M.; Cádiz V. A renewable approach to thermosetting resins. React. Funct. Polym. 2013; 73: 381–95.

[22] Montero de Espinosa L.; Meier M. A.R. Plant oils: The perfect renewable resource for polymer science?!. Eur. Polym. J. 2011; 47: 837–52.

[23] Xia Y.; Larock R. C. Vegetable oil-based polymeric materials: synthesis, properties, and applications. Green Chem. 2010; 12: 1893–909.

[24] Sharma V.; Kundu P. P. Addition polymers from natural oils-A review. Prog. Polym. Sci. 2006; 31: 983–1008.

[25] Ogunniyi D. S. Castor oil: A vital industrial raw material, Bioresour. Technol. 2006; 97: 1086–91.

[26] López Téllez G.; Vigueras-Santiago E.; Hernández-López S. Characterization of linseed oil epoxidized at different percentages. Superficies y Vacío 2009; 22: 5–10.

[27] Lu J., Khot S., Wool R. P. New sheet molding compound resins from soybean oil. I. Synthesis and characterization. Polymer 2005; 46: 71–80.

[28] Lu J.; Wool R. P. Novel thermosetting resins for SMC applications from linseed oil: Synthesis, characterization, and properties. J. Appl. Polym. Sci. 2006; 99: 2481–8.

[29] Xia Y.; Henna P. H.; Larock R. C. Novel Thermosets from the Cationic Copolymerization of Modified Linseed Oils and Dicyclopentadiene. Macromol. Mater. Eng. 2009; 294: 590–8.

[30] Montero de Espinosa, L.; Ronda, J. C.; Galià, M.; Cádiz, V. A new enone-containing triglyceride derivative as precursor of thermosets from renewable resources. J. Polym. Sci. Part A: Polym. Chem. 2008; 46: 6843–50.

[31] Montero de Espinosa,; Ronda L.; J. C.; Galià, M.; Càdiz, V. Quinoline-Containing Networks from Enone and Aldehyde Triglyceride. J. Polym. Sci. Part A: Polym. Chem. 2010; 48: 869–78.

[32] De Espinosa L. M.; Ronda J. C.; Galia M.; Cadiz V. A Straightforward Strategy for the Efficient Synthesis of Acrylate and Phosphine Oxide-Containing Vegetable Oils and Their Crosslinked Materials. J. Polym. Sci. Part A: Polym. Chem. 2009; 47: 4051–63.

[33] Barto R. R.; Frank C. W.; Bedworth P. V.; Taylor R. E.; Anderson W. W.; Ermer S., et al. Bonding and Molecular Environment Effects on Near-Infrared Optical Absorption Behavior in Nonlinear Optical Monoazo Chromophore-Polymer Materials. Macromolecules 2006; 39: 7566–77.

[34] Bucio E.; Burillo G.; Carreón-Castro M. del P.; Ogawa T. Functionalization of Polypropylene Film by Radiation Grafting of Acryloyl Chloride and Subsequent Esterification with Disperse Red 1. J Appl Polym Sci. 2004; 93: 172–8.

[35] Kade M. J.; Burke D. J.; Hawker C. J. The Power of Thiol-ene Chemistry. J. Polym. Sci. Part A: Polym. Chem. 2010; 48: 743–50.

[36] Hoyle C. E.; Bowman C. N. Thiol–Ene Click Chemistry. Angew. Chem. Int. Ed. 2010; 49: 1540–73.

[37] Hayashi T.; Thornton P. D. The synthesis and characterisation of thiol-bearing C. I. Disperse Red 1. Dyes Pigm. 2015; 121: 235–7.

[38] Sheehan J.; Cruickshank P.; Boshart G. J. Org. Chem. 1961; 26: 2525–8.

[39] Lluch C.; Lligadas G.; Ronda J. C.; Galià M.; Cadiz V. "Click" Synthesis of Fatty Acid Derivatives as Fast-Degrading Polyanhydride Precursors. Macromol. Rapid Commun. 2011; 32: 1343–51.

[40] Bantchev G. B.; Kenar J. A.; Biresaw G.; Han M. G. Free Radical Addition of Butanethiol to Vegetable Oil Double Bonds. J. Agric. Food Chem.

2009; 57: 1282–90.

[41] Claudino M.; Johansson M; Jonsson M. Thiol–ene coupling of 1,2-disubstituted alkene monomers: The kinetic effect of cis/trans-isomer structures. Eur. Polym. J. 2010; 46: 2321–32.

[42] Sacchi R.; Addeo F.; Paolillo L. ^{1}H and ^{13}C NMR of Virgin Olive Oil. An overview. Magn. Reson. Chem. 1997; 35: S5133–45.

[43] Uygun M.; Tasdelen M. A.; Yagci Y. Influence of Type of Initiation on Thiol–Ene "Click" Chemistry. Macromol. Chem. Phys. 2010; 21: 103–10.

[44] Cinara M.; Coruhc A.; Karabacak M. FT-IR, UV–vis, ^{1}H and ^{13}C NMR spectra and the equilibrium structure of organic dye molecule disperse red 1 acrylate: A combined experimental and theoretical analysis Spectrochem. Acta. A. 2011; 83: 561–9.

[45] Tuman S.J.; Chamberlain D.; Scholsky K. M.; Soucek M. D. Differential scanning calorimetry study of linseed oil cured with metal catalysts. Prog. Org. Coatings. 1996; 28: 251–8.

[46] Baylon A.; Stauffer É; Delémont O. Evaluation of the Self-Heating Tendency of Vegetable Oils by Differential Scanning Calorimetry. J. Forensic. Sci. 2008; 53: 1334–43.

[47] Cui Y; Wang M.; Chen L.; Qian G. Synthesis and spectroscopic characterization of an alkoxysilane dye containing C. I. Disperse Red 1. Dyes Pigm. 2004; 62: 43–7.

7. Graphical Abstract
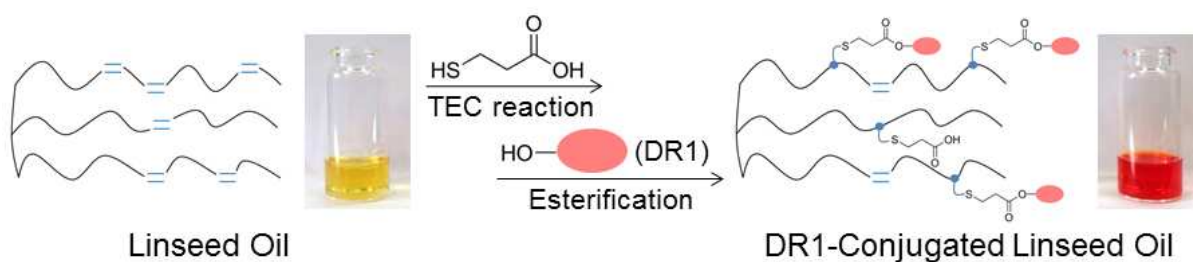
Dye conjugation to linseed oil by highly-effective thiol-ene coupling

and subsequent esterification reactions

SUPPLEMENTARY INFORMATION

Toshiki Hayashi[1], Algy Kazlauciunas[2] and Paul D Thornton[2*]

1. National Printing Bureau of Japan, Odawara, Kanagawa 256-0816, Japan.

2. School of Chemistry, University of Leeds, Leeds, LS2 9JT, UK.

Email: p.d.thornton@leeds.ac.uk

1. Quantification of the Reactions

The quantification of reactions 1 and 2 were conducted by monitoring changes in the intensities of selected peaks found on ^{1}H NMR spectra, as follows:

(1) Reaction 1

The conversion ratios of C=C bonds reacting with **2** were calculated from the decrease in the peak area in the region of 5.3 ppm ($I_{5.3 \text{ ppm}}$) (Fig. 2). $I_{5.3 \text{ ppm}}$ is composed of the peak from the vinylic protons on the C=C carbons (g) (I_g) and the proton from the glycerol unit (a) (I_a). Given, all molecules in **1** are triglyceride,

$$I_{5.3 \text{ ppm}} = I_g + I_a \tag{1}$$

One triglyceride molecule includes one C<u>H</u>COO proton (a) (1H), and four C<u>H</u>$_2$COO protons (b) (4H). The intensities of the latter protons were normalised to 4.00, enabling each peak intensity on the ^{1}H NMR chart to represent the number of hydrogen atoms in one triglyceride molecule. Thus, the intensities of vinylic protons (g) in the region of 5.3 ppm become:

$$I_g = I_{5.3 \text{ ppm}} - 1 \tag{2}$$

Then, the number of C=C bonds in one triglyceride molecule ($N_{C=C}$) becomes

$$\begin{aligned} N_{C=C} &= I_{\underline{HC=CH}} / 2 \\ &= (I_{5.3 \text{ ppm}} - 1) / 2 \end{aligned} \tag{3}$$

Thus, the conversion ratio of reaction 1 (X_1) is represented as

$$X_1 = [(N_{C=C})_{\text{before reaction}} - (N_{C=C})_{\text{after reaction}}] \times 100 / (N_{C=C})_{\text{before reaction}} \quad [\%] \tag{4}$$

By using X_1, the average number of functional groups (COOH) on one triglyceride molecule (N_{COOH}) and the average molecular weight of **3** (M) are expressed as follows

$$N_{COOH} = (N_{C=C})_{\text{before reaction}} X_1 \tag{5}$$

$$M = M_1 + M_2 N_{COOH} \quad [\text{g/mol}] \tag{6}$$

where M_1 (= 873.60 g/mol), is the average molecular weight of linseed oil as reported in the literature [10], and M_2 (= 106.14 g/mol) is the molecular weight of **2**.

24

(2) Reaction 2

The quantification of reaction 2 was also conducted with ^{1}H NMR as follows (Fig. 7). The peaks from the protons of the C$\underline{H}_2$COO units (b) which are from **3** (4H) are found at both 4.0–4.1 ppm and 4.2–4.3 ppm at equal intensities. Also, the peaks from the protons of the C$\underline{H}_2$COO units, which are from **4** (2H) conjugated to **3** (o′), are found at 4.2–4.3 ppm. By comparing both peaks at 4.2–4.3 ppm, the average number of **4** (DR1) molecules conjugated to one **3** molecule (N_{DR1}) is calculated as follows.

$$
\begin{aligned}
N_{DR1} &= [(I_{o'})_{\mathbf{4}} / 2] / [(I_b)_{\mathbf{3}} / 4] \\
&= [(I_{4.2–4.3\ \text{ppm}} - I_{4.0–4.1\ \text{ppm}}) / 2] / (I_{4.0–4.1\ \text{ppm}} \times 2 / 4) \\
&= [I_{4.2–4.3\ \text{ppm}} - I_{4.0–4.1\ \text{ppm}}] / I_{4.0–4.1\ \text{ppm}}
\end{aligned} \tag{7}
$$

Thus, the conversion ratio of reaction 2 (X_2) is represented as

$$
X_2 = (N_{DR1} / N_{COOH}) \times 100 \quad [\%] \tag{8}
$$

and the overall conversion ratio (X_{overall}) is represented as

$$
X_{\text{overall}} = [N_{DR1} / (N_{C=C})_{\text{before reaction}}] \times 100 \quad [\%] \tag{9}
$$

25

2. HMQC

HQMC charts of (a) **1** and (b) **3** (No. 12 obtained in reaction 1) are shown in Fig. SI 1.

(a)

(b)
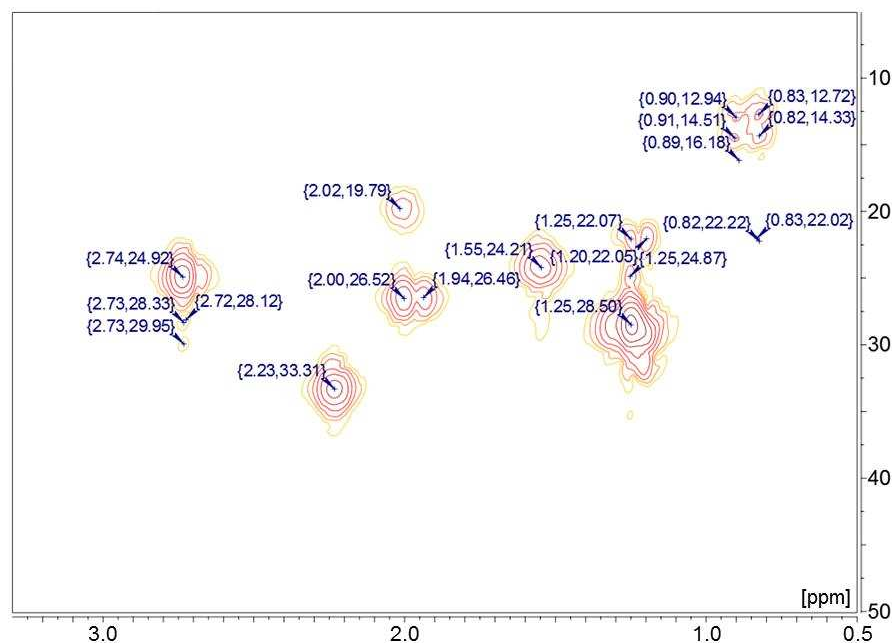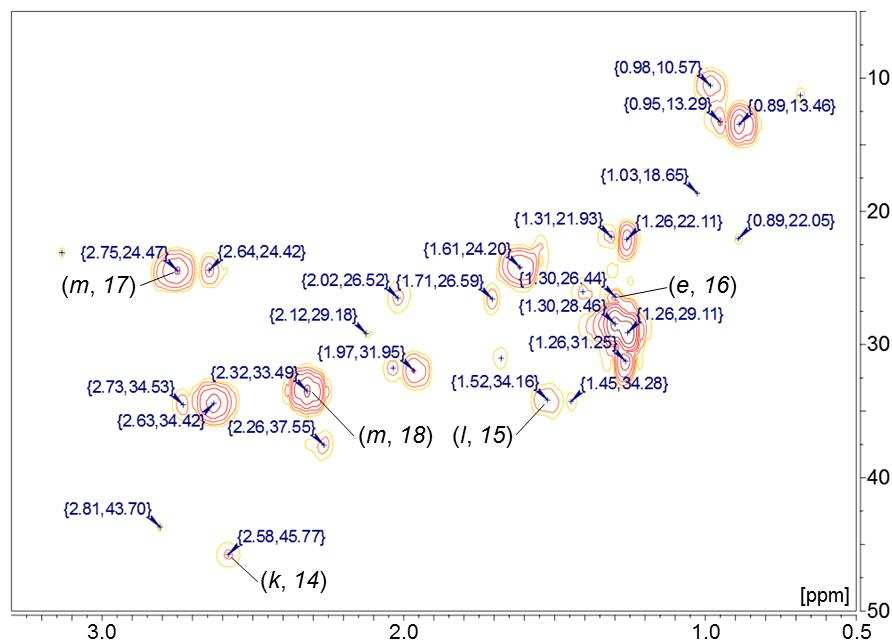
Fig. SI 1 HQMC charts of (a) **1** and (b) **3** (No. 12 obtained in reaction 1). A magnified view of the range of 0.5–3.3 ppm (^{1}H NMR), and the range of 5–50 ppm (^{13}C NMR). Assignments were done for characteristic peaks which signify the formation of the C-S bond in reaction 1. Alphabetical letters and figures in the brackets signify the assignments of protons (as in Fig. 2) and carbon atoms (as in Fig. 6), respectively.

3. Thermal Properties

TGA and DSC results of 3 with different conversion ratios are summarised in Table SI 1, and shown in Fig. SI 2 and Fig. SI 3, respectively.

Table SI 1. Thermal Properties of **3** with different conversion ratios.

Samples[*1]	TGA	DSC	
	T_d [°C]	T_m [°C]	T_p [°C]
Modified Linseed Oil (**3**) (No. 2)	347.2	−11.1	−60.0
3 (No. 3)	329.7	−10.9	−48.2
3 (No. 4)	313.7	−10.3	−40.1
3 (No. 6)	303.7	−9.1	−33.4
3 (No. 9)	295.8	−7.0	−31.2
3 (No. 12)	286.6	−3.9	−27.9

T_d: thermal decomposition temperature, T_m: melting temperature, T_p: phase transition temperature, λ_{max}: maximum absorption wavelength. [*1] Obtained in reaction 1. Conversion ratios of each sample are shown in Table 1.
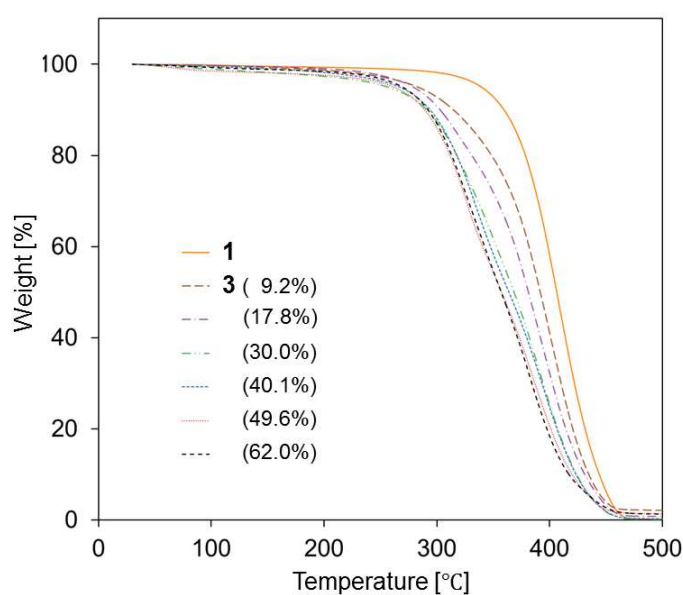
Fig. SI 2 TGA curves of **1** and **3** with different conversion ratios.
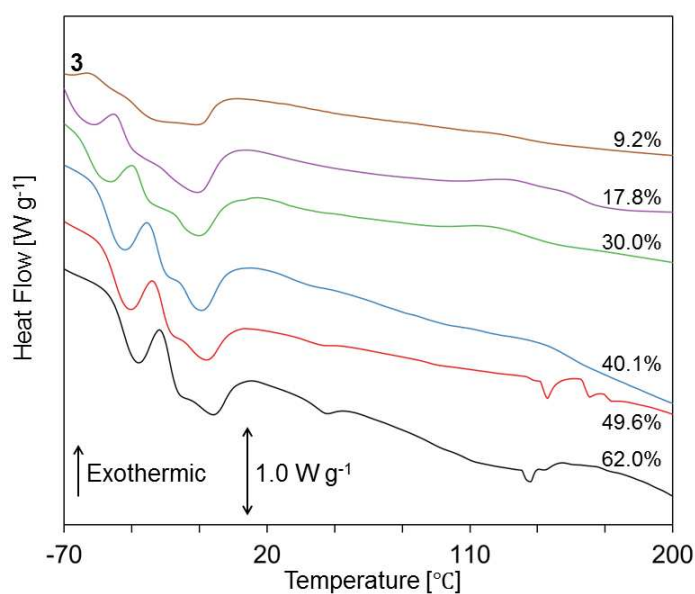
Fig. SI 3 DSC curves of **3** with different conversion ratios.

27